High Performance Photo-Induced Substrate-Integrated Waveguide for Tunable and Reconfigurable THz Circuits

Y. J. Deng*, M. I. B. Shams, J. Ren, P. Fay, and L. Liu
Department of Electrical Engineering, University of Notre Dame, Notre Dame, IN 46556, USA
*Contact: ydeng2@nd.edu

Abstract— **We present a novel approach for realizing tunable/reconfigurable THz circuits using photo-induced substrate-integrated waveguide (PI-SIW) architectures. In this approach, fixed metallic vias in conventional SIW are replaced by photo-induced conductive plasma sidewalls. Full-wave HFSS simulation has shown an insertion loss of 4.15 dB/mm at 280 GHz with photo-induced sidewalls formed by 80 W/cm² light intensity (550 nm wavelength) on high resistivity silicon (HRS) wafer. To further improve the PI-SIW performance, a pillar-array structure is proposed to suppress carrier diffusion while same time increasing the achievable photoconductivity. With such pillar-array structures, the insertion loss at 280 GHz has been reduced to as low as 0.96 dB/mm, and a value of 0.81 dB/mm can be potentially achieved for a 300 W/cm² light intensity.**

I. Introduction

Recently, electromagnetic waves in the THz region have attracted increased interests owing to the promising applications in radio astronomy, medical imaging, security screening, high-speed communication and defense. Tunable and reconfigurable THz circuits have become highly desired in advanced THz sensing, imaging and adaptive wireless communication systems. A variety of approaches such as mechanical tuning [1], thermal agitation [2], electrical tuning using Schottky or PIN diodes [3-4], and metamaterial approaches [5] have been reported to demonstrate THz tunable/reconfigurable components. However, most of those approaches rely on prepatterned circuits, resulting in limited tunability and versatility. In addition, more advanced THz tunable circuits such as phase shifters, delay lines, high-level switches (e.g., SPDT, DPDT) are still quite challenging to realize.

In this paper, we report an alternative approach for realizing the above tunable/reconfigurable THz circuits using photo-induced substrate-integrated waveguide (PI-SIW) architectures. On the basis of the optical THz spatial modulation (OTSM) technology reported in our previous work [6, 7], fixed metallic vias in conventional SIW structures can be replaced with conductive plasma SIW sidewalls by projecting programmable light patterns on semiconductors. For a prototype demonstration, a PI-SIW structure with a height of 100 um and width of 285 um was designed using HRS to achieve the fundamental mode cut-off frequency of 150 GHz. Commercial FEM solver ANSYS-HFSS was utilized for circuit simulation. Simulated results showed an insertion loss of 4.15 dB/mm at 280 GHz with photo-induced sidewalls formed by 80 W/cm² light intensity (550 nm wavelength). This high insertion loss is primarily attributed to relatively low photoconductivity achieved and inclined sidewalls due to lateral carrier diffusion. To further improve the PI-SIW performance, a pillar-array structure was applied to suppress carrier lateral diffusion (for straight sidewalls) while same time increasing the achievable photoconductivity. With the proposed pillar-array structure, the insertion loss of a PI-SIW at 280 GHz can be reduced to as low as 0.96 dB/mm, and a value of 0.81 dB/mm can be potentially achieved for a 300 W/cm² light intensity. The PI-SIW structures proposed and reported in this paper have low insertion loss and strong reconfigurability, making them promising for achieving tunable/reconfigurable circuits for advanced THz sensing, imaging and communication.

II. PI-SIW Architectures

A Demonstration of PI-SIW Structures

In the PI-SIW structures, fixed metallic vias in conventional SIWs are replaced with conductive plasma SIW sidewalls by projecting programmable light patterns on semiconductors, as is illustrated in Fig. 1. The vertical carrier concentration profile and photoconductivity of silicon wafer illuminated by continuous waves can be calculated from the well-known expressions in [7]. A thin layer of indium tin oxide (ITO) was used to replace the top conductor in a conventional SIW for fulfilling such regional illumination using a combination of a DMD chip and a laser source.

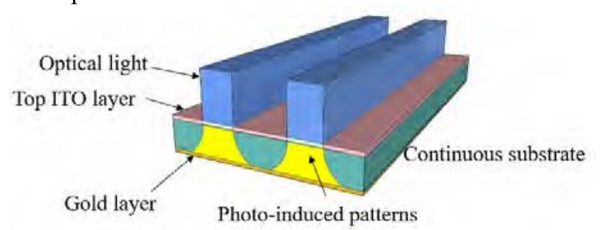

Fig. 1. PI-SIW on continuous HRS substrate

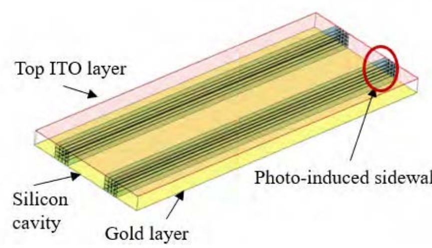

Fig. 2. PI-SIW structure on continuous HRS substrate in HFSS

For a prototype demonstration, 80 W/cm^2 light intensity is used to illuminate on continuous HRS wafer [8]. As shown in Fig. 2, PI-SIW with a height of 100 μm, width of 285 μm and length of 2 mm was designed using full-wave HFSS.

Nevertheless, optical light illuminating on continuous HRS substrate will cause inclined sidewalls due to lateral carrier diffusion as illustrated in Fig. 3. Consequently, such PI region displays relatively low and inconsistent carrier concentration. Being able to inhibit lateral diffusion of carriers will improve the spatial resolution of the photopatterns, while at the same time increase the photo-induced carrier concentration and maintain high modulation speed. Based on this purpose, pillar-array structure, a matrix of isolated islands each with lateral dimension well below the THz wavelength (at the operating frequency), is introduced. Photo-induced substrate with pillar-array structure in Fig. 3 constrains photogenerated carriers within every single pillar and reduces lateral carrier diffusion. A much higher free carrier concentration as well as photoconductivity can thus be achieved in PI regions with pillar arrays.

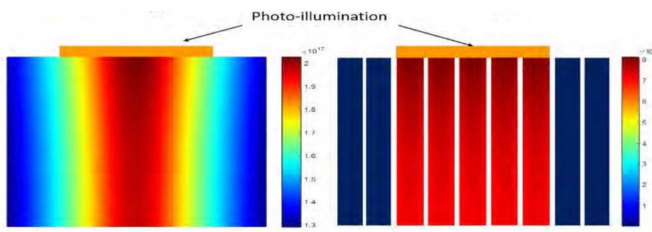

(a) (b)

Fig. 3. Photo-induced substrate (a) without and (b) with pillar-array structure

For the verification of PI-SIW structure demonstrated in Fig. 4 (a), pillar arrays were devised with unit size of 10 um x 10 um, trench width of 0.5 um and SIW cavity length of 986.5 um. SIW structure was redesigned in ANSYS-HFSS with the aforementioned pillar-array design.

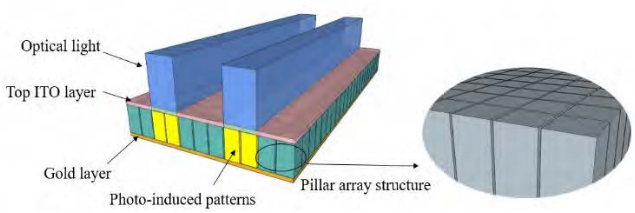

(a) (b)

Fig. 4. (a) PI-SIW structure with (b) pillar-array structure

B PI-SIW Simulated Results and Discussion

First, PI-SIW on continuous HRS substrate is simulated in ANSYS-HFSS. The continuous PI sidewalls are formed with a light intensity of 80 W/cm^2. An insertion loss of 4.15 dB/mm is observed at 280 GHz in Fig. 5. Such high insertion loss is primarily attributed to relatively low photoconductivity achieved and inclined sidewalls due to lateral carrier diffusion.

Subsequently, for the performance prediction of pillar-array structures, PI-SIW on continuous HRS substrate with pillar-array sidewalls are simulated. This is an extreme and ideal circumstance when the width of pillar-array trenches goes to zero while remains the abovementioned properties of pillar-array construction. As shown in Fig. 5, the corresponding insertion loss under light intensity of 80 W/cm^2, 100 W/cm^2, 200 W/cm^2, 300 W/cm^2 are 1.50 dB/mm, 1.38 dB/mm, 0.94 dB/mm, 0.81 dB/mm respectively. Under the light intensity of 80 W/cm^2, the insertion loss of PI-SIW with pillar-array sidewalls at 280 GHz is ~2.6 dB/mm superior than that of PI-SIW with continuous sidewalls. By increasing optical light intensity, photoconductivity of pillar-array sidewalls is increased and the insertion loss of PI-SIW structure is consequently diminished. An insertion loss as low as 0.81 dB/mm can be achieved by PI-SIW with pillar-array sidewalls at a light intensity of 300 W/cm^2.

Finally, a practicable structure for fabrication and measurements, PI-SIW with pillar-array construction, is simulated in ANSYS-HFSS. As displayed in Fig. 5, the insertion loss is 0.96 dB/mm at 280 GHz with a light intensity of 300 W/cm^2, which is only ~0.15 dB/mm inferior than its extreme case where trench width is zero and the substrate becomes continuous. The shifting of cutoff frequency (~4 GHz) is caused by an equivalent permittivity lower than silicon due to air-filling trenches. The E-field distribution of proposed PI-SIW with pillar-array configuration is given in Fig. 6.

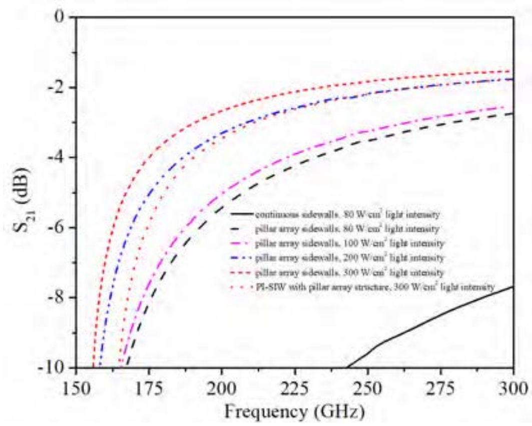

Fig. 5. S-parameter frequency responses for PI-SIW structures under light intensity of 80 W/cm^2, 100 W/cm^2, 200 W/cm^2, 300 W/cm^2 (transmission line length of 2 mm)

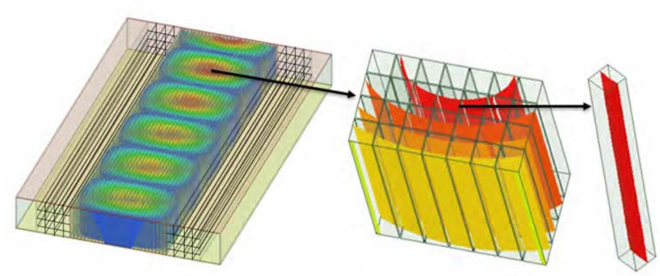

Fig. 6. Electric field distribution of PI-SIW with pillar-array structure and its zoom-in figures

CONCLUSIONS AND FUTURE WORKS

A novel approach for realizing tunable/reconfigurable THz circuits using photo-induced substrate-integrated waveguide (PI-SIW) architectures is reported in this work. Full-wave HFSS simulation has shown an insertion loss of 4.15 dB/mm at 280 GHz with PI sidewalls formed by 80 W/cm^2 light intensity. Such high insertion loss is attributed to relatively low photoconductivity achieved and inclined sidewalls due to lateral carrier diffusion. Pillar-array construction is therefore introduced to constrain photogenerated carriers within every isolated pillar and suppress lateral carrier diffusion. Simulated results indicate that the insertion loss of PI-SIW with pillar-array structure can be reduced to as low as 0.96 dB/mm, and a value of 0.81 dB/mm can be achieved with 300 W/cm^2 light intensity. The proposed high-performance PI-SIW has huge potential in more advanced THz tunable/ reconfigurable circuits such as phase shifters, delay lines and high-level switches (e.g. SPDT, DPDT).

On the basis of the above work: THz tunable circuit designs based on the proposed high-performance PI-SIW structures with pillar arrays will soon be designed and simulated. Meanwhile, pillar-array technique for realizing high resolution circuits and components will be fabricated. For SIW measurements, SIW-to-CPW transitions will be devised and fabricated. Furthermore, on-wafer measurements using THz VNAs and probe station systems for the performance of the developed circuits based on PI-SIWs will be conducted.

Acknowledgment

This work is partially supported by the National Science Foundation (NSF) under the grant of ECCS-1711631 and ECCS-1711052, and a subcontract from the Harvard-Smithsonian Center for Astrophysics under grant PTX-Smithsonian 17-SUBC-400SV787007. The authors would like to thank the support from Center for Nano Science and Technology (NDnano) and Advanced Diagnostics & Therapeutics (AD&T) at the University of Notre Dame.

References

[1] J. Li et al, “Mechanically tunable terahertz metamaterials,” Appl. Phys. Lett., vol. 102, no.12, 2013, Art. ID 121101.

[2] L. Liu et al, “Temperature control of terahertz metamaterials with liquid crystals,” IEEE Trans. THz Sci. Technol., vol. 3, no. 6, pp. 827-831, 2013.

[3] Z. Jiang, S. M. Rahman, P. Fay, J. L. Hesler and L. Liu, “Tunable 200 GHz lens-coupled annular-slot antennas using Schottky varactor diodes for all-electronic reconfigurable terahertz circuits,” Electronics Letters, vol. 49, no. 23, p. 1428 – 1430, 2013.

[4] S. Preu, G. H. Döhler, S. Malzer, L. J. Wang, and A. C. Gossard, “Tunable, continuous-wave Terahertz photomixer sources and applications,” J. Appl. Phys., vol. 109, no.6, 2011, Art. ID 061301.

[5] J. Wu et al., “Tuning of superconducting niobium nitride terahertz metamaterials,” Opt. Express, vol. 19, no. 13, p. 11922 (1-6), 2011.

[6] L. Cheng and L. Liu, “Optical modulation of continuous terahertz waves towards cost-effective reconfigurable quasi-optical terahertz components,” Opt. Exp., vol. 21, no. 23, pp. 28657-28667, 2013.

[7] A. Kannegulla, M. I. B. Shams, L. Liu, and L.-J. Cheng, “Photo-induced spatial modulation of THz waves: opportunities and limitations,” Opt. Exp., vol. 23, no. 25, pp.32098-32112, 2015.

[8] Y. Zhou and S. Lucyszyn, “Modelling of reconfigurable terahertz integrated architecture SIW structures,” Prog. Electromagn. Res., vol. 105, pp. 71–92, 2010